

Supporting Information for:

# Flexibility and Swing Effect on the Adsorption of Energy-Related Gases in ZIF-8: Combined Experimental and Simulation Study

David Fairen-Jimenez,<sup>a,d,\*</sup> Raimondas Galvelis,<sup>b</sup> Antonio Torrisi,<sup>b</sup> Alistair Gellan,<sup>a</sup> Michael T. Wharmby,<sup>c</sup> Paul A. Wright,<sup>c</sup> Caroline Mellot-Draznieks<sup>b</sup> and Tina Düren<sup>a</sup>

<sup>a</sup>Institute for Materials and Processes, School of Engineering, The University of Edinburgh, United Kingdom; <sup>b</sup>Department of Chemistry, University College London, United Kingdom; <sup>c</sup>EaStCHEM School of Chemistry, University of St. Andrews, United Kingdom; <sup>d</sup>Current address: Department of Chemical and Biological Engineering, Northwestern University, USA.

\*To whom correspondence should be addressed. E-mail: David.Fairen-Jimenez@Northwestern.edu

## Table of contents

Section S1. ZIF-8 structure: Pore size distribution and partial charges.....	1
Section S2. Gas adsorption on ZIF-8.....	3
Section S3. DFT minimization of CH <sub>4</sub> on ZIF-8AP.....	8
Section S4. DFT minimization of CH <sub>4</sub> on ZIF-8HP.....	10

## Section S1. Pore size distribution and partial charges of ZIF-8

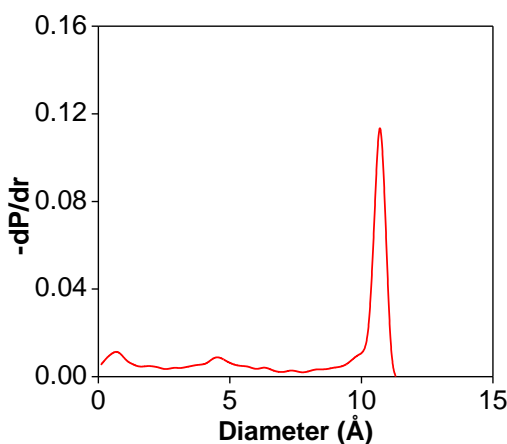


**Figure S1.** Pore size distribution (PSD) for the ZIF-8 structure.

**Table S1:** Point charges on Imidazole ligand in ZIF-8 and in isolated molecule, extracted from DFT (PBE) calculation (Mulliken charges).

	Imidazole (fig. A)	Cluster (fig. B)	Periodic (fig.C)
N	-0.358	-0.459	-0.403
N	-0.323	-0.422	-0.403
C <sub>double</sub>	0.020	0.061	0.004
C <sub>double</sub>	-0.003	0.019	0.004
C <sub>NN</sub>	0.277	0.374	0.317
C <sub>methyl</sub>	-0.304	-0.302	-0.358
H <sub>double</sub>	0.070	0.050	0.107
H <sub>double</sub>	0.076	0.078	0.107
H <sub>methyl</sub>	0.105	0.102	0.147
H <sub>methyl</sub>	0.109	0.100	0.147
H <sub>methyl</sub>	0.131	0.148	0.147
H <sub>(N)</sub>	0.200	-	-
Zn	-	0.361	0.367
Zn	-	0.378	0.367

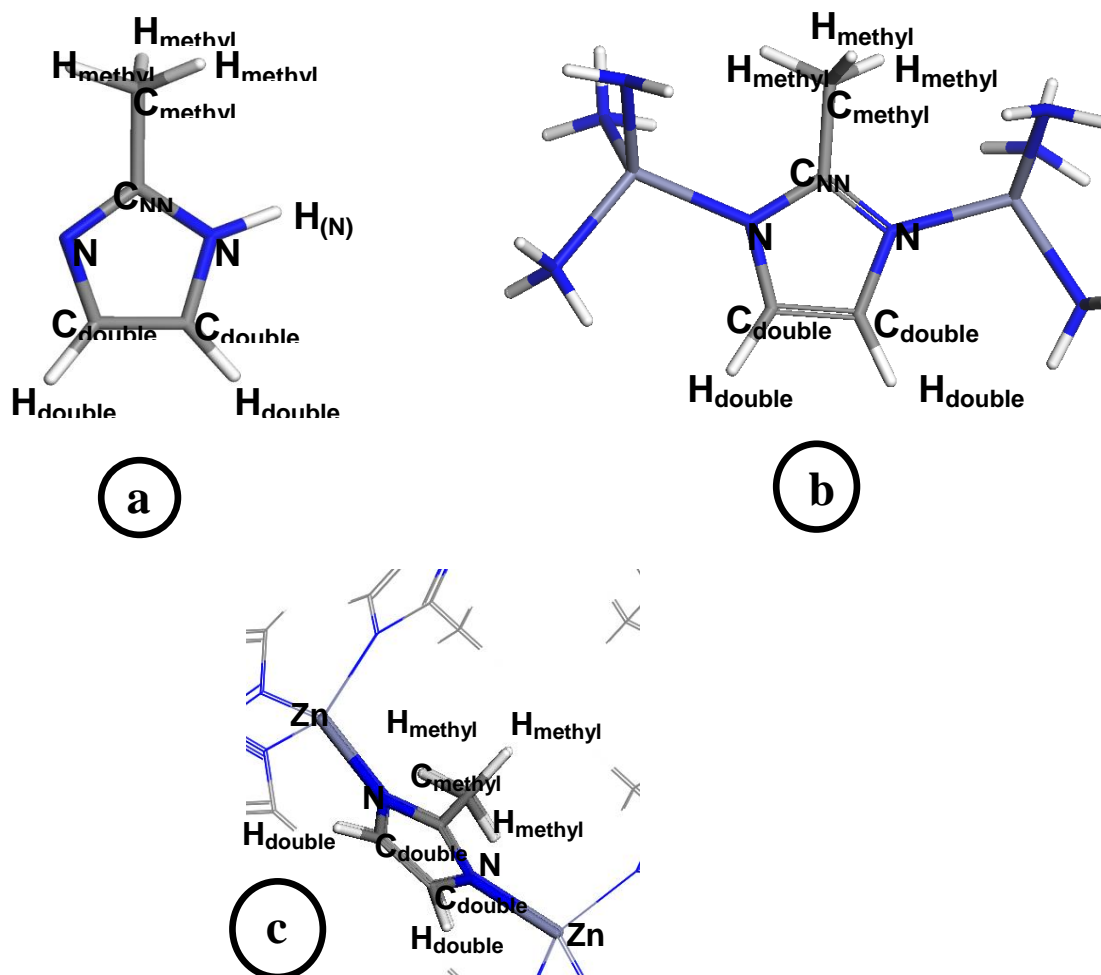


**Figure S2:** a) Imidazole, b) cluster and c) periodic boundary conditions representations for the extraction of Mulliken charges.

## Section S2. Gas adsorption on ZIF-8.

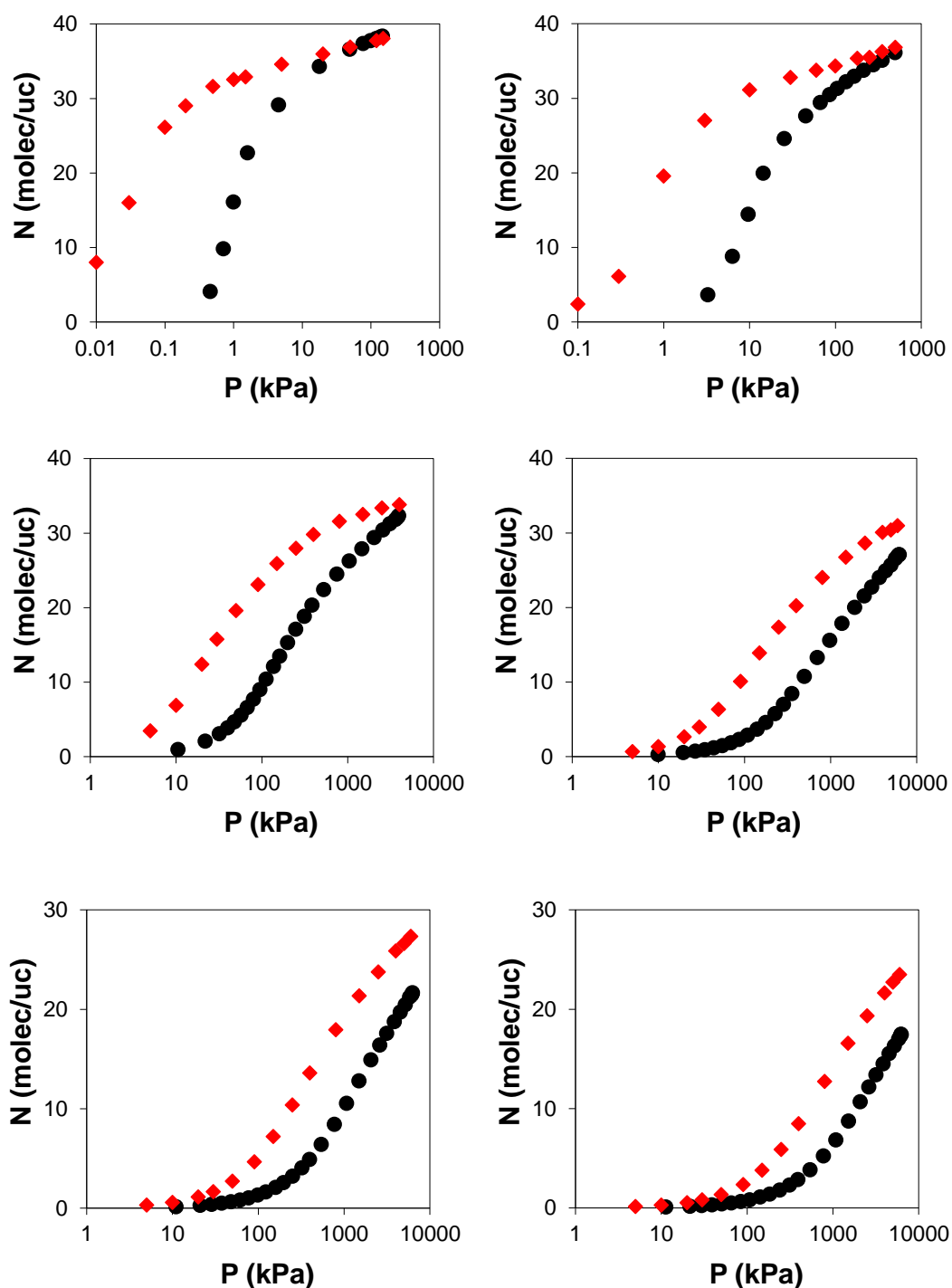


**Figure S3.** Adsorption isotherms of methane on ZIF-8 at (from top-left to bottom-right) 125, 150, 200, 240, 270 and 300 K. Experiments, black circles; UFF simulations on ZIF-8AP, red diamonds.

**Table S2.** Scaling factors ( $\phi$ ) applied to UFF-simulated isotherms of methane on ZIF-8AP in order to match experimental maximum amount adsorbed for isotherms at different temperatures.

Temperature (K)	125	150	200	230	270	300
$\phi$	1.01	0.98	0.96	0.88	0.79	0.74

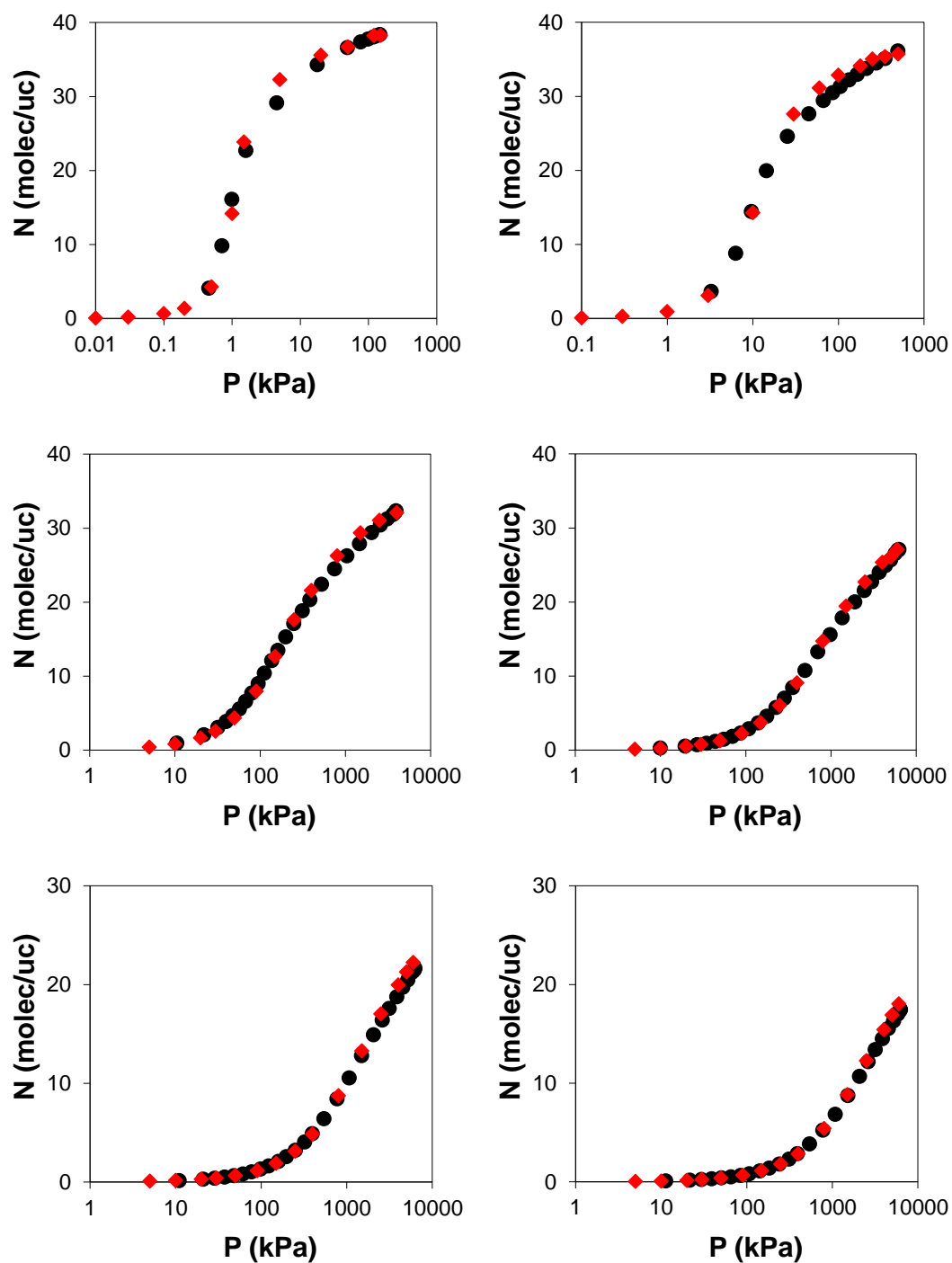


**Figure S4.** Adsorption isotherms of methane on ZIF-8 at (from top-left to bottom-right) 125, 150, 200, 240, 270 and 300 K. Experiments, black circles; UFF(\*) simulations on ZIF-8AP, red diamonds.

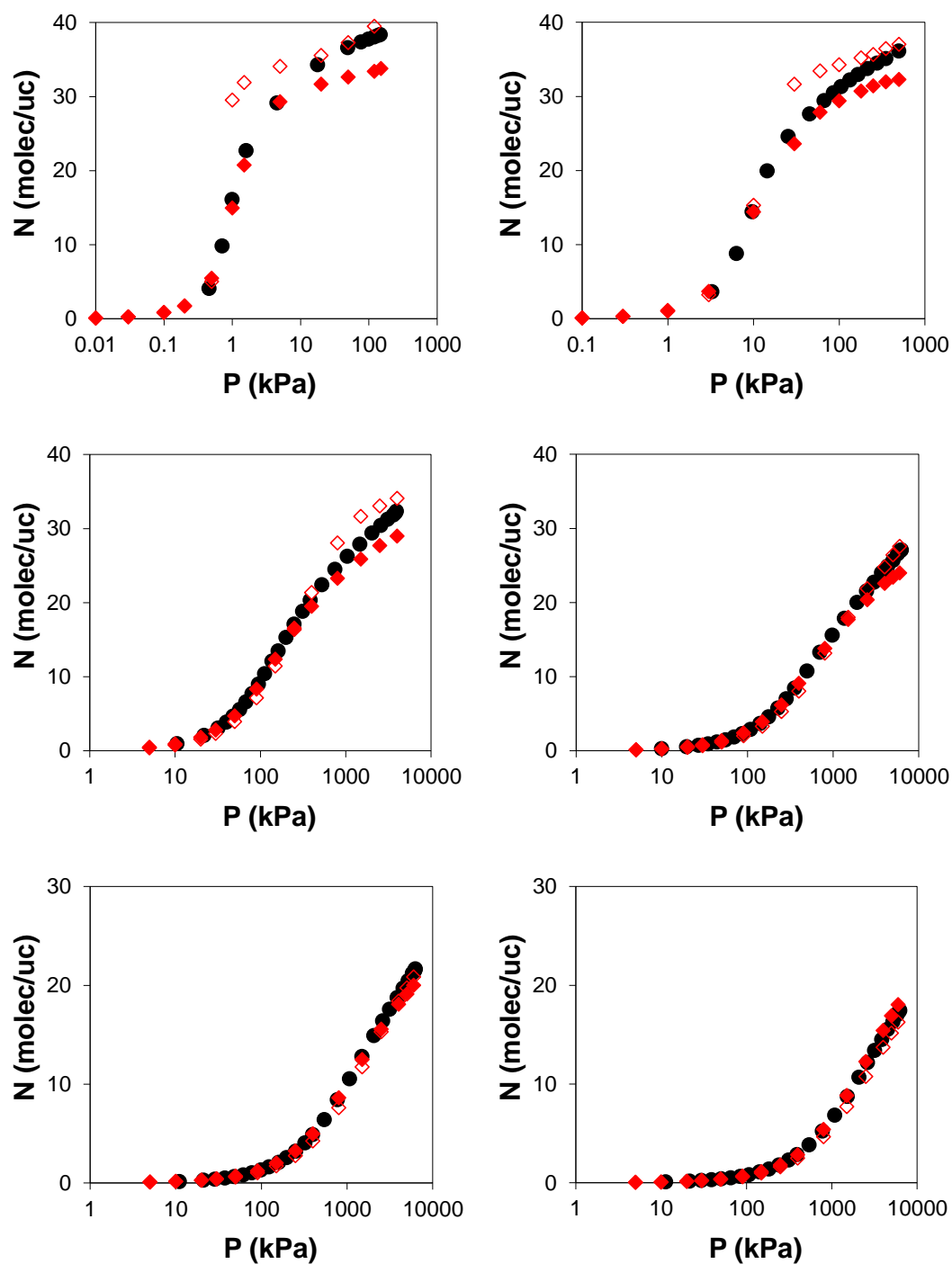


**Figure S5.** Adsorption isotherms of methane on ZIF-8 at (from top-left to bottom-right) 125, 150, 200, 240, 270 and 300 K. Experiments, black circles UFF(+) on ZIF-8AP, closed red diamonds; UFF(+) on ZIF-8HP, open red diamonds

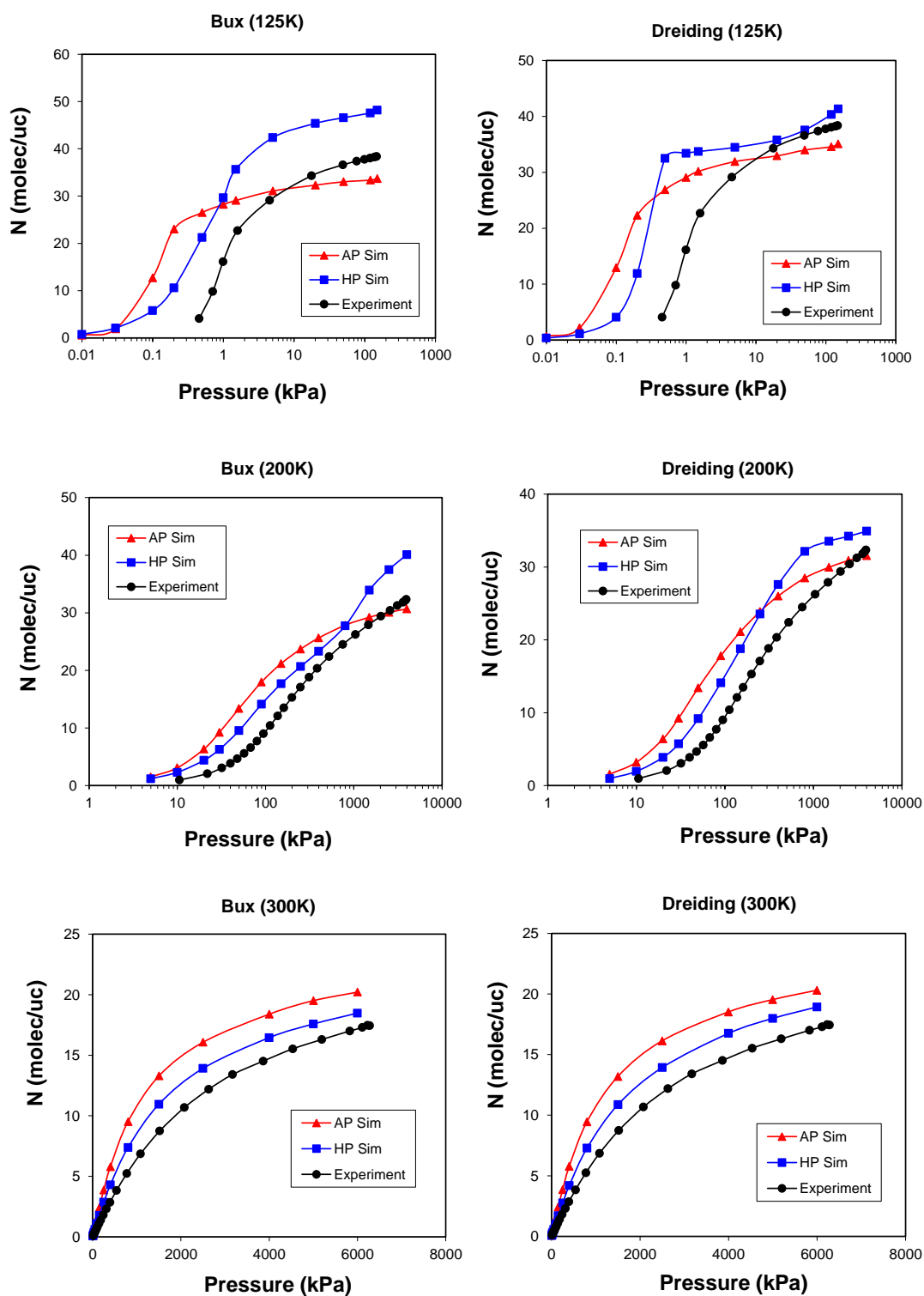


**Figure S6.** Adsorption isotherms of methane on ZIF-8 at 125, 200 and 300 K. Experiments, black circles; (left) Bux et al force field, and (right) Dreiding force field. ZIF-8AP, red triangles; ZIF-8HP, blue squares.

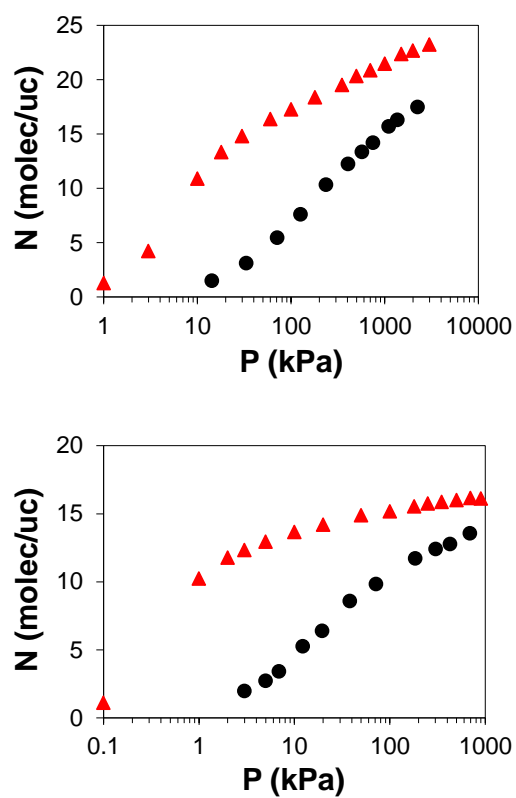


**Figure S7.** Adsorption isotherms of (from top to bottom) ethane and propane on ZIF-8 at 273 K. Experiments, black circles UFF on ZIF-8AP, closed red triangles.

### Section S3. DFT minimization on CH<sub>4</sub> in ZIF-8AP.

**Configuration  $\alpha_2$ :** The second most stable configuration (Figure S8) has BE of  $-17.2 \text{ kJ mol}^{-1}$  and it corresponds to CH<sub>4</sub> located on top of the C=C double bond, with H(CH<sub>4</sub>) $\cdots$ C=C distances of  $\sim 2.8 \text{ \AA}$ , likewise the most stable configuration  $\alpha_1$  (Figure 6).

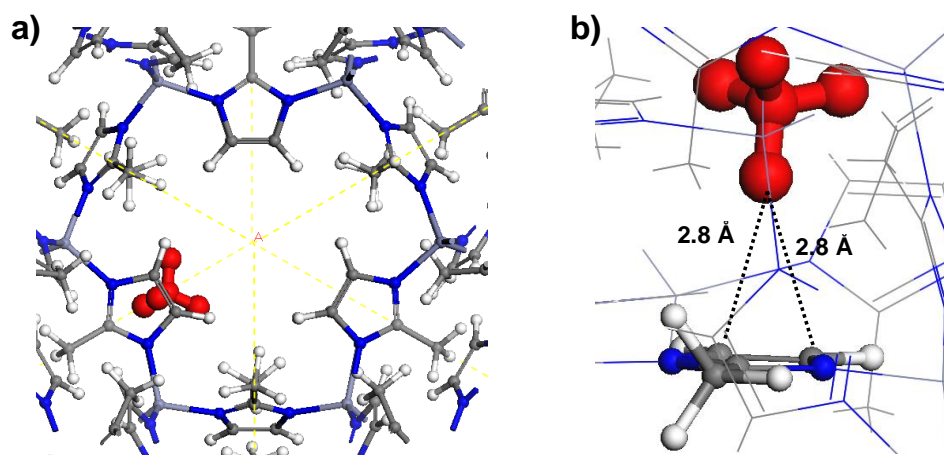


**Figure S8** Configuration  $\alpha_2$  for one CH<sub>4</sub> in ZIF-8AP, resulting from energy minimizations with DFT calculations with Grimme dispersive correction.

**Configuration  $\alpha_3$ :** Very similar to the most stable configuration (configuration  $\alpha_1$ ), with CH<sub>4</sub> on top of C=C double bond of imidazole ligand with one hydrogen pointing towards the double bond, having binding energy BE =  $-16.4 \text{ kJ mol}^{-1}$  (Figure S9). As in configuration  $\alpha_2$ , the short H(CH<sub>4</sub>) $\cdots$ C=C distances are of  $\sim 2.8 \text{ \AA}$ .

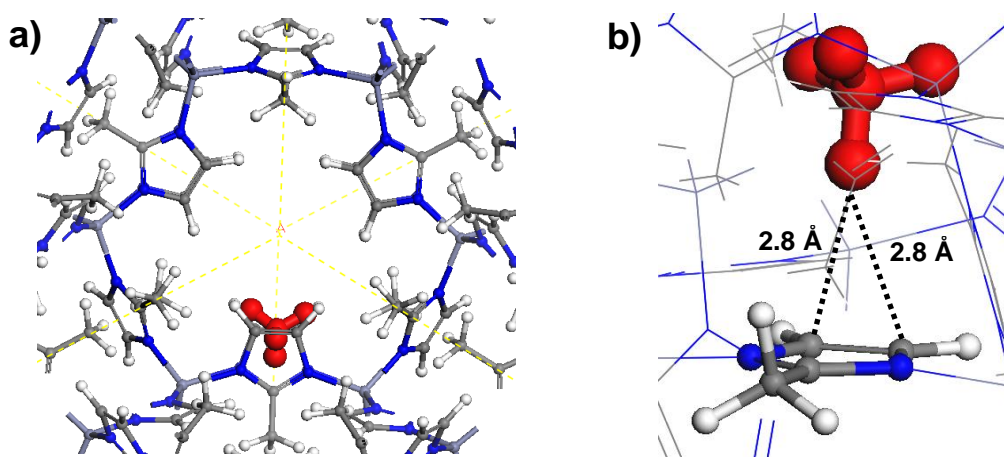


**Figure S9:** Configuration  $\alpha_3$  for one CH<sub>4</sub> in ZIF-8AP, resulting from energy minimizations with DFT calculations with Grimme dispersive correction.



**Configuration  $\beta_2$ :** The fifth stable configuration with BE of  $-16.0 \text{ kJ mol}^{-1}$  is characterised by  $\text{CH}_4$  located at the centre of the 6-ring pore-window, similar to configuration  $\beta_1$ , with  $\text{H}(\text{CH}_4)\cdots\text{C}=\text{C}$  distance of  $2.9 \text{ \AA}$  (Figure S10). The peculiar feature of this configuration when compared with configuration  $\beta_1$ , is the absence of weak interactions between  $\text{H}(\text{CH}_4)$  and the  $-\text{CH}_3$  groups of imidazolate, as indicated by the relatively long  $\text{H}(\text{CH}_4)\cdots\text{C}(\text{CH}_3)$  distances of  $5.3 \text{ \AA}$ . Likewise at Site I, the main interaction of  $\text{CH}_4$  with the ZIF-8AP framework occurs with the  $\text{C}=\text{C}$  double bond of the imidazolate ring, including an additional contribution of weak interactions with the  $-\text{CH}_3$  groups of the imidazolate linker on  $\beta_1$ , which are not present on  $\beta_2$ . Indeed, this is clearly shown by the DFT calculations, where the differences between  $\beta_1$  and  $\beta_2$  are about  $2 \text{ kJ mol}^{-1}$  in BE. Another important difference between the two configurations is the position of  $\text{CH}_4$  along the perpendicular axis to the 6-ring window (Figure 7 and S10). In fact, in configuration  $\beta_1$ ,  $\text{CH}_4$  is located above this plane, outside the “sodalite” central cage of ZIF-8AP, facilitating the interaction of the  $\text{H}(\text{CH}_4)$  with the  $-\text{CH}_3$  groups of imidazolate linker. On the other hand, in configuration  $\beta_2$ , methane is located below the plane, within the “sodalite” central cage of ZIF-8AP, and far from the  $-\text{CH}_3$  groups of imidazolate, whose interaction with  $\text{CH}_4$  is prevented.

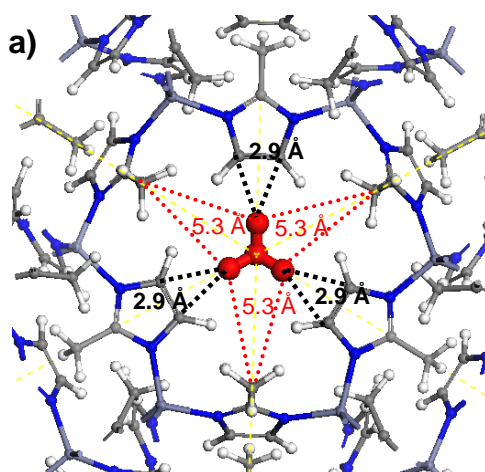


**Figure S10:** Configuration  $\beta_2$  for one  $\text{CH}_4$  in ZIF-8AP, resulting from energy minimizations with DFT calculations with Grimme dispersive correction.

#### Section S4. DFT minimization on CH<sub>4</sub> in ZIF-8HP.

**Table S3.** Mülliken charge ( $\Delta q$ ) variation for CH<sub>4</sub> species in the different adsorption sites of ZIF-8AP and ZIF-8HP, with respect to the isolated molecule.  $\Delta q = q(\text{CH}_4 \text{ in ZIF-8HP}) - q(\text{CH}_4 \text{ isolated})$ .

	$\Delta q_{\text{TOT}}$ (CH <sub>4</sub> )	$\Delta q(\text{C})$	$\Delta q(\text{H})$	$\Delta q(\text{H})$	$\Delta q(\text{H})$	$\Delta q(\text{H})$
<b>ZIF-8AP</b>						
$\alpha_1$	-0.0025	-0.0074	-0.0041	+0.0128	-0.0025	-0.0013
$\alpha_2$	+0.0035	+0.0000	-0.0024	-0.0032	+0.0116	-0.0025
$\alpha_3$	+0.0038	+0.0006	-0.0023	-0.0025	+0.0113	-0.0033
$\beta_1$	+0.0146	-0.0041	-0.0049	-0.0041	-0.0041	-0.0041
$\beta_2$	-0.0044	+0.0076	-0.0057	+0.0049	-0.0056	-0.0056
$\gamma$	+0.0005	+0.0006	-0.0002	+0.0002	+0.0001	-0.0002
<b>ZIF-8HP</b>						
$\Theta$	-0.0266	+0.0139	+0.0032	+0.0029	+0.0032	+0.0034